DOI: 10.1002/masy.200751009

Comparative Study of Scattering and Osmotic Properties of Synthetic and Biopolymer Gels

Ferenc Horkay,[*1] *Peter J. Basser,*[1] *Anne-Marie Hecht,*[2] *Erik Geissler*[2]

Summary: The effect of monovalent/divalent cation exchange on the structure and osmotic properties of chemically cross-linked polyacrylate and DNA gels swollen in near physiological salt solutions has been investigated. Both systems exhibit a reversible volume phase transition in the presence of calcium ions. The small-angle neutron scattering spectra of these gels display qualitatively similar features. At low values of q surface scattering is observed, while in the intermediate q range the signal is characteristic of scattering from rod-like elements. At high values of q the scattering intensity is governed by the local (short-range) geometry of the polymer chains. The competition between monovalent and divalent cations has been studied by anomalous small-angle X-ray scattering (ASAXS). The ASAXS results reveal that the local concentration of the divalent counter-ions in the vicinity of the polymer chains significantly exceeds that of the monovalent counter-ions.

Keywords: anomalous X-ray scattering; biopolymers; gels; ion distribution; small-angle neutron scattering

Introduction

Ions are implicated in a wide-range of physiological processes.[1,2] The structure, dynamics and the corresponding biological properties of charged biopolymers (e.g., DNA, proteins) cannot be fully understood without taking into account solvent hydration and the ionic atmosphere surrounding the molecules. It is known that, when the concentration of multivalent cations is increased, many polyelectrolytes undergo a volume transition from a swollen to a collapsed state.[3–5] The ability of DNA to undergo dramatic conformation transitions is important in gene therapy, because large extended molecules cannot be delivered into the cells.[6] Study of the thermodynamic and structural aspects of ion/polymer interactions has the potential to contribute to a more comprehensive understanding of the mechanism of ion-mediated structural organization of charged biomacromolecules.

Biological materials operate at cell and subcellular dimensions; therefore, physical properties such as osmotic and mechanical properties, state of hydration, and charge density must be characterized on distance scales below 1000 Å. What is unique about these materials is that, rather than the local molecular configuration, the long-range polymer structures are most likely to be the key to their physical behavior. A promising approach seems to be to apply to biopolymer systems methodologies that have been developed and tested on synthetic polymers. Small-angle scattering methods, both small-angle neutron scattering (SANS) and small-angle X-ray scattering (SAXS), are essential for characterizing the conformation and hierarchical organization of macromolecules as a function of the length scale.[7]

In this paper we compare the effect of ions on the osmotic and scattering behavior

[1] Section on Tissue Biophysics and Biomimetics, National Institute of Child Health and Human Development, National Institutes of Health, 13 South Drive, Bethesda, MD 20892, USA
E-mail: horkay@helix.nih.gov
[2] Laboratoire de Spectrométrie Physique CNRS UMR 5588, Université J. Fourier de Grenoble, B.P. 87, 38402 St Martin d'Hères cedex, France

of a biological and a synthetic polyelectrolyte gel: DNA and polyacrylic acid. Both gels exhibit a reversible volume transition in near-physiological salt solutions as the concentration of divalent ions (in the present case calcium ions) increases. Scattering measurements alone would not allow us to separate the contributions arising from thermodynamic concentration fluctuations from that of frozen-in by the permanent cross-links. The latter considerably affects the shape of the scattering curve, particularly at low values of the scattering vector. To overcome the difficulty associated with the evaluation of the scattering experiment in terms of thermodynamic quantities, we made osmotic swelling pressure measurements on both gel systems to estimate the thermodynamic concentration fluctuations independently. Furthermore, an attempt was made to determine the distribution of monovalent and divalent counter-ions in the ion cloud around the polyelectrolyte molecules in the course of the ion exchange process. These measurements were made in hyaluronic acid (HA) solutions using anomalous small-angle X-ray scattering (ASAXS). In principle, this technique allows us to distinguish between counter-ions associated with the polymer chains and those in the bulk solution.

Theory

Small-angle scattering measurements (SANS and SAXS) probe length scales in the range of 10-1000 Å and determine the organization of the polymer chains.[7] In the SANS experiment, the intensity of neutrons scattered by atomic nuclei is measured, while in SAXS the incident photons interact with electrons, and provide information about the fluctuations of electronic densities in the heterogeneous matrix.

The scattering vector (momentum transfer) is defined by the formula

$$q = \frac{4\pi}{\lambda}\sin\theta \tag{1}$$

where λ is the neutron wavelength and 2θ is the scattering angle. The intensity scattered from a semidilute solution of flexible polymer chains can be described by an Ornstein-Zernike type equation[8]

$$I_{os}(q) = \frac{I_{os}(q=0)}{1+q^2\xi^2} \tag{2}$$

where ξ is the polymer-polymer correlation length. The intensity at $q=0$ (thermodynamic limit) is directly related to the osmotic modulus, K_{os}, of the solution

$$K_{os} = \varphi\frac{\partial\Pi}{\partial\varphi} \tag{3}$$

where Π is the osmotic pressure of the solution and φ is the volume fraction of the polymer.

In gels chemical cross-links create permanent structural nonuniformities that contribute strongly to the scattering intensity[9–11]

$$I(q) = I_{os}(q) + I_{cr}(q) \tag{4}$$

where $I_{cr}(q)$ is the scattering contribution of the frozen-in regions.

Many important biopolymers are electrically charged and are best represented as semi-rigid chains. For gels made of rod-like molecules the total scattering intensity can be described by[12]

$$I(q) = \Delta\rho^2\frac{k_BT\varphi^2}{M_{os}}\frac{1}{(1+qL)(1+q^2r_c^2)} + Aq^{-m} \tag{5}$$

where $\Delta\rho^2$ is the neutron contrast factor, M_{os} is the longitudinal osmotic modulus, L is the rod-length and r_c is the cross-sectional radius of the polymer molecule. In Equation 5 the second term describes the excess static scattering observed in polyelectrolytes at low values of q. A and m are constants.[13,14]

Materials and Methods

Sample Preparation

Sodium polyacrylate (PAA) gels were prepared by free-radical copolymerization of acrylic acid and N,N′-methylenebis (acrylamide) cross-linker in aqueous solution according to a procedure described

previously.[15] The monomer concentration was 30% (w/w), and 35% of the acrylic acid monomers were neutralized by sodium hydroxide prior to polymerization. The crosslinking process was carried out at 80 °C.

DNA gels were made from deoxyribonucleic acid sodium salt (Sigma).[16] The % G-C content of the DNA was 41.2%. The molecular weight determined by ultracentrifugation was 1.3×10^6 Da, which corresponds to approximately 2000 base pairs. DNA gels were made by cross-linking with ethyleneglycol diglycidyl ether in solution [pH = 9.0, $c_{DNA} = 3\%$ (w/w)]. TEMED was used to adjust the pH.

Sodium hyaluronate (HA, Sigma $M_w = 1.2 \times 10^6$ Da) was dissolved at room temperature in 100 mM NaCl at pH = 7. The HA concentration of the solution was 4% (w/w). HA solutions were also prepared in 100 mM RbCl. Divalent salt concentrations, $CaCl_2$ or $SrCl_2$, were varied from 0 to 100 mM, while the concentrations of the polymer and monovalent salts were kept constant.

Small-Angle Neutron Scattering Measurements

SANS measurements were made in D_2O on the NG3 instrument at NIST, Gaithersburg, MD, using an incident wavelength $\lambda = 8$ Å. The transfer wave vector explored in the experiments covered the range $0.003\ \text{Å}^{-1} < q < 0.2\ \text{Å}^{-1}$. After azimuthal averaging, corrections for incoherent background, detector response and cell window scattering were applied.[17]

ASAXS Measurements

The ASAXS measurements were made on the BM2 beam line at the European Synchrotron Radiation Facility (ESRF). The transfer wave vector range explored was $0.008\ \text{Å}^{-1} \leq q \leq 1.0\ \text{Å}^{-1}$. The measured intensities were normalized using a standard polyethylene sample (lupolen) of known scattering cross-section. To limit radiation damage effects, sequences of exposure times were limited to 20 s and the position of the beam in the sample was changed at each successive energy. The SAXS measurements were made at six energies below the absorption edge (15.1997 keV) of rubidium: 14.900, 15.08, 15.15, 15.18, 15.193 and 15.197 keV, and at six energies below the absorption edge (16.1046 keV) of strontium: 15.800, 15.984, 16.056, 16.085, 16.097 and 16.102 keV.

Osmotic Measurements

Osmotic swelling pressure measurements were made on gels using a method described elsewhere.[18] Gels were equilibrated with aqueous solutions of poly(vinyl pyrrolidone) (PVP, molecular weight: 29 kDa) of known osmotic pressure.[19] The gels were separated from the polymer solution by a semi-permeable membrane (dialysis bag) to prevent penetration of the PVP molecules into the swollen network.

Elastic Modulus Measurements

Uniaxial compression measurements were made on cylindrical gel samples in equilibrium with salt solutions using a TA.XT2I HR Texture Analyser (Stable Micro Systems, UK). This apparatus measures the uniaxial deformation (±0.001 mm) as a function of the applied force (±0.01 N). All measurements were made at 25 ± 0.1 °C.

Results and Discussion

Ion-induced Phase Transition in Gels

Figure 1 shows the variation of the swelling degree as a function of the $CaCl_2$ concentration in the equilibrium 40 mM NaCl solution for a DNA and a PAA gel. Gel swelling decreases with increasing Ca ion concentration. Divalent cations screen the repulsive forces between the negatively charged groups on the polymer backbone and influence the hydration properties of the polymer molecule. In both gels a discontinuous volume transition can be observed at a critical threshold concentration of the $CaCl_2$, i.e., the gel shrinks and solvent is expelled.

In Figure 2 is illustrated the variation of the osmotic swelling pressure as a function

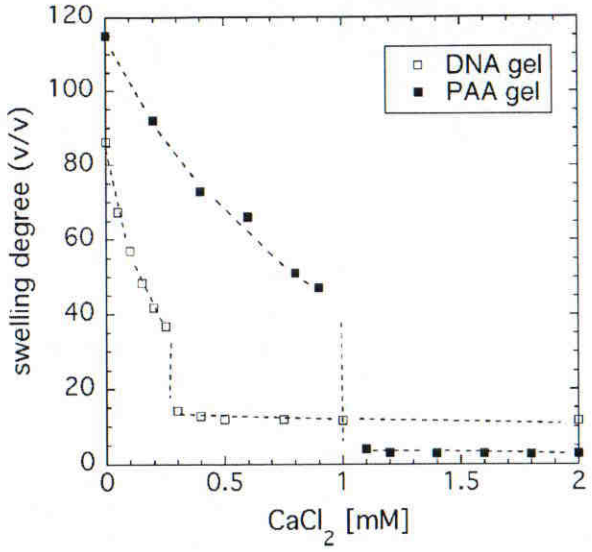

Figure 1.
Variation of the swelling degree with the $CaCl_2$ concentration for DNA and PAA gels swollen in 40 mM NaCl solution.

of the polymer concentration for the same DNA and PAA gels shown in Figure 1. During the osmotic measurements the $CaCl_2$ concentration of the surrounding solutions was held constant. The decrease of the swelling pressure with increasing $CaCl_2$ concentration indicates that Ca ions favor the formation of clusters and ultimately lead to phase separation. At and above the phase transition the chemical potential of the solvent in the coexisting phases is identical.

Figure 3 shows the SANS response of a DNA gel (NaCl concentration: 40 mM,

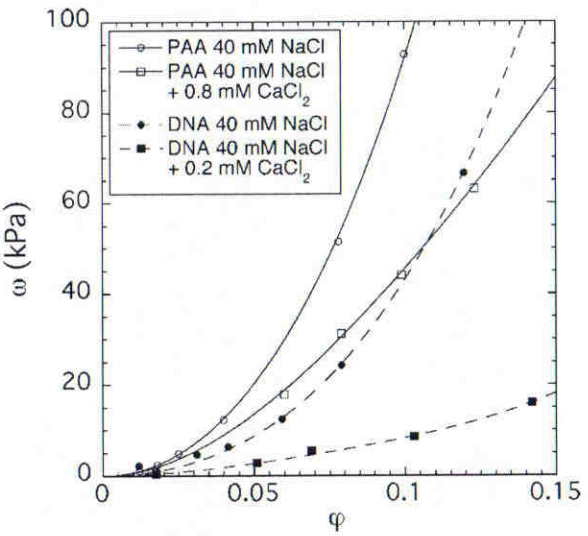

Figure 2.
Dependence of the osmotic swelling pressure on the polymer volume fraction for PAA and DNA gels swollen in 40 mM NaCl solution containing different amounts of $CaCl_2$.

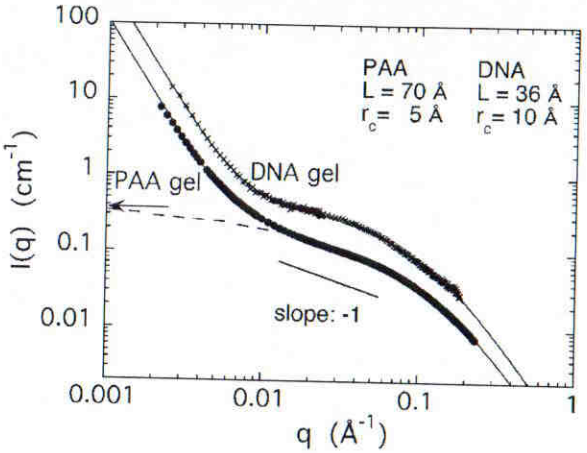

Figure 3.
SANS intensity from DNA and PAA gels in 40 mM NaCl solution containing $CaCl_2$. (DNA gel: 0.25 mM $CaCl_2$, PAA gel: 0.8 mM $CaCl_2$). Continuous lines: fit of Equation 5 to the SANS data. Dashed line: osmotic component (first term of Equation 5) of the fit. Arrow: intensity of the osmotic concentration fluctuations calculated from macroscopic measurements.

$CaCl_2$ concentration: 0.25 mM) and a polyacrylate gel (NaCl concentration: 40 mM, $CaCl_2$ concentration: 0.8 mM). The scattering curves look similar despite major differences between the chemical structure of the two polymers. At low q a power law behavior is visible with an exponent $-3.6 < m < -4$ characteristic of scattering from surfaces. At intermediate q a component that varies as q^{-1} is distinguishable. This behavior is typical of scattering from rod-like elements. At high q the scattering response can be described by the Ornstein-Zernike type expression. The continuous curves through the SANS data points are the least squares fits of Equation 5 to the data. The dashed curve shown for the PAA gel is the osmotic component of this fit (first term in Equation 5).

In gels the osmotically driven concentration fluctuations are controlled by the longitudinal osmotic modulus[20,21]

$$M_{os} = \varphi \frac{\partial \omega}{\partial \varphi} + \frac{4}{3} G \qquad (6)$$

where ω is the osmotic swelling pressure and G is the shear modulus. M_{os} can be calculated independently from macroscopic measurements of ω and G.

Equation 5 and 6 provides a means to compare the thermodynamic component of the SANS spectrum and the amplitude of the osmotically driven concentration fluctuations estimated from macroscopic measurements. According to Equation 5 the intensity scattered by the thermal fluctuations is proportional to φ^2/M_{os}. In Figure 3 the horizontal arrow at the left axis shows the scattering intensity due to thermodynamic concentration fluctuations calculated from independent osmotic and mechanical measurements (at $q = 0$) for the PAA gel. Reasonable agreement is found between the scattering intensities obtained from the two entirely different and independent techniques.

Determination of the Counter-ion Distribution

An understanding of ion-polymer interactions in polyelectrolyte solutions and gels requires knowledge of the counter-ion distribution. We made anomalous small-angle X-ray scattering (ASAXS) measurements to study the ion distribution in the ionic atmosphere surrounding the charged macromolecules. In the ASAXS experiment the energy of the incident radiation is varied in the vicinity of the absorption edge

of the counter-ion. In this way the effective electron density and thus the scattering contrast between the counter-ions and the solvent gradually vary, while the contrast between the polymer and the solvent remains unchanged. The difference between the scattering intensities from the same sample at two different incident energies E_1 and E_2 is given by

$$\begin{aligned}\Delta I(q, E_1, E_2) &= I(q, E_1) - I(q, E_2) \\ &= 2r_0^2[(\Delta f'/v_c) \\ &\quad \times \{b_p S_{cp}(q) \\ &\quad + (b_c - \Delta f'/2v_c) S_{cc}(q)\} \\ &\quad + \{f''^2(E_2) - f''^2(E_1)\} S_{cc}(q)/2v_c^2] \end{aligned} \quad (7)$$

where r_0 (2.818×10^{-13} cm) is the radius of the electron. $b_p = (\rho_p\text{-}\rho_s)$ and $b_c = (\rho_c(E)\text{-}\rho_s)$ are the difference in electron density between the polymer (p) and solvent (s) and between the counter-ion cloud (c) and solvent, respectively, $S_{jk}(q)$ are the partial structure factors, in which j and k represent either the polymer or the ion cloud, and v_c is the volume of the counter-ion. f_0, f' and f'' are respectively the energy-independent number of electrons, and the real and imaginary number of energy-dependent electrons in the counter-ion, and $\Delta f' = f'(E_1) - f'(E_2)$.

We made ASAXS measurements on HA solutions. HA is a well suited model biopolymer to investigate the ionic cloud, particularly the competition between monovalent and divalent cations, since its static structure is relatively insensitive to the presence of high valence counter-ions. In the ASAXS experiment the physiologically relevant monovalent and divalent cations were replaced by rubidium and strontium ions, because the absorption edge of the latter ions (Rb: 15.199 keV, Sr: 16.102 keV) lies in the energy range conveniently accessible for synchrotron measurements.

Figure 4 illustrates the effect of the energy of the incident photons on the scattering contrast of a HA solution containing 100 mM RbCl. The data measured at three different energies are plotted in the representation $qI(q)$ *vs* q in order to make the differences more visible. As the incident X-ray energy increases towards the absorption edge of rubidium, the scattering intensity decreases. At low q the higher energy measurements lie below the spectrum measured at 14.9 keV. (At 14.9 keV the anomalous scattering effects are

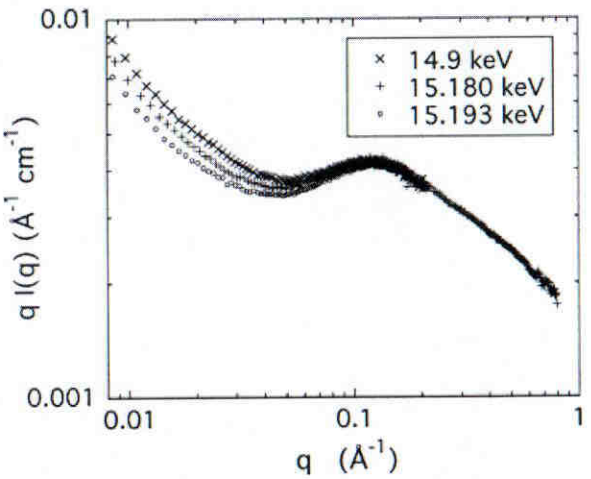

Figure 4.
Plot of $qI(q)$ for 4% solutions of divalent ion-free RbHA solutions at three different incident X-ray energies below the Rb threshold.

negligible.) However, at high q the differences among the data tend to vanish.

We investigated the effect of divalent ions on the counter-ion distribution in two complementary configurations. In the first (Sr/Na system) the ASAXS signal was due to the strontium ions, while in the second (Rb/Ca system) the rubidium was the resonant species. In both configurations the monovalent cation concentration was set at 100 mM and the concentration of the divalent cations was varied from 0 to 100 mM.

It has been shown[22,23] that the relative scattering amplitude of the counter-ion cloud is given by

$$\alpha_c(q) = \Delta I(q)/[I(q)]^{1/2} \quad (8)$$

According to Equation 8, the scattering amplitude is defined by the difference between the spectra measured at two energies, normalized by the square root of the reference signal. The intensities should be measured far below the absorption edge and that just below the edge, where the anomalous effects are most pronounced.[22,24] The resulting scattering amplitude $\alpha_c(q)$ is the Fourier transform of the ion cloud and its functional form reflects the shape and radial extent of the counter-ion distribution.

Figure 5 shows the dependences of the anomalous amplitudes $\alpha_c(q)$ measured at $q = 0.01$ Å^{-1}, in both configurations. In the Sr/Na systems (circles), in which Sr ions compete with sodium ions, the effect of saturation in the divalent/monovalent ion exchange process is clearly visible. In the Ca/Rb system (squares) $\alpha_c(q)$ weakly decreases as the $CaCl_2$ concentration increases, implying that the thickness of the rubidium ion cloud gradually decreases with increasing calcium concentration, but it does not vanish completely. Even when the divalent ion concentration exceeds the stoichiometric concentration by more than an order of magnitude, the monovalent counter-ion cloud is still detectable.

The relative concentration of the divalent cations can be estimated on the basis of the cell model. In this model the polymer chain is approximated as a cylindrical rod with a uniform surface charge density. The counter-ion concentration at the cell limit plays an analogous role as the bulk concentration. The radius of the cell corresponding to the present 4% HA solution is approximately 27 Å. The HA molecule has an inner core with a radius of 5.2 Å that is impermeable to the ions. The outer radius of the divalent ion shell is approximately 7.5 Å. Let us assume that in

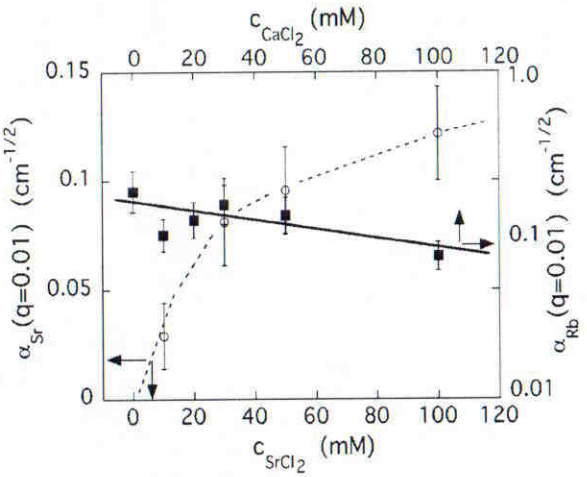

Figure 5.
Scattering amplitudes $\alpha_{Sr}(q = 0.01)$ and $\alpha_{Rb}(q = 0.01)$ of Sr and Rb anomalous signals at $q = 0.01$ Å^{-1} as a function of $SrCl_2$ and $CaCl_2$ concentrations of the solution.

the case of the Sr/Na system the fraction of sites occupied by Sr ions is 50%. In a solution containing 50 mM cations this yields for the ratio of the Sr ion concentration within the shell to that outside it equal to 50. This result implies that divalent counter-ions replace the majority of the monovalent counter-ions even if their concentration is much lower, and tend to be preferentially adsorbed on the negative sites of the polymer chain. It can be seen from Figure 5 that the competition between monovalent and divalent cations begins at low divalent ion concentration (below 10 mM $SrCl_2$). Most noticeable changes in the amounts of adsorbed Sr ions are observed between 5 and 30 mM.

Conclusions

SANS and osmotic measurements performed on chemically cross-linked polyacrylate and DNA gels swollen in near physiological salt solutions indicate similarities between the physico-chemical properties of these polymers. Addition of calcium ions to both systems induces a reversible volume phase transition. The SANS response reveals the presence of large clusters, the size of which exceeds the resolution of the SANS experiment, i.e., 1000 Å. At intermediate values of q the logarithm of the scattering intensity decreases linearly with the logarithm of q. This scattering response is characteristic of rod-like structural elements. At high values of q the scattering intensity is governed by the local (short-range) geometry of the polymer chains.

The results of anomalous small-angle X-ray scattering measurements indicate that the concentration of the divalent counter-ions in the vicinity of the polymer chains significantly exceeds that of the monovalent counter-ions. At concentrations close to that of biological media, the monovalent ions are pushed out of this region by divalent cations even if the concentration of the divalent ions is much lower.

Acknowledgements: This research was supported by the Intramural Research Program of the NICHD/NIH. We acknowledge the National Institute of Standards and Technology, U.S. Department of Commerce in providing the neutron research facilities used in this experiment. This work utilized facilities supported in part by the National Science Foundation under Agreement No. DMR-0454672. We are grateful to the European Synchrotron Radiation Facility for access to the French CRG X-ray beam line BM2.

[1] I. Tasaki, P. M. Byrne, *Biopolymers* **1994**, *34*, 209.
[2] I. Tasaki, *Jpn. J. Physiol.* **1999**, *49*, 125.
[3] A. Katchalsky, S. Lifson, H. Eisenberg, *J. Polym. Sci.* **1951**, *7*, 571.
[4] A. Katchalsky, I. Michaeli, *J. Polym. Sci.* **1955**, *15*, 69.
[5] J. Ricka, T. Tanaka, *Macromolecules* **1984**, *17*, 2916.
[6] V. A. Bloomfield, *Biopolymers* **1977**, *44*, 269.
[7] J. S. Higgins, H. C. Benoit, "*Polymers and Neutron Scattering*", Clarendon Press, Oxford **1994**.
[8] P. G. de Gennes, "*Scaling Concepts in Polymer Physics*", Cornell University Press, Ithaca, NY **1979**.
[9] F. Horkay, A. M. Hecht, S. Mallam, E. Geissler, A. R. Rennie, *Macromolecules* **1991**, *24*, 2896.
[10] E. Geissler, F. Horkay, A. M. Hecht, *Phys. Rev. Lett.* **1993**, *71*, 645.
[11] F. Horkay, P. J. Basser, A. M. Hecht, E. Geissler, *Polymer* **2005**, *46*, 4242.
[12] F. Horkay, I. Grillo, P. J. Basser, A. M. Hecht, E. Geissler, *J. Chem. Phys.* **2002**, *117*, 9103.
[13] K. S. Schmitz, M. Lu, J. Gaunnt, *J. Chem. Phys.* **1983**, *78*, 5059.
[14] J. J. Tanahatoe, M. E. Kuil, *J. Phys. Chem. B* **1997**, *101*, 9233.
[15] F. Horkay, I. Tasaki, P. J. Basser, *Biomacromolecules* **2000**, *1*, 84.
[16] F. Horkay, P. J. Basser, *Biomacromolecules* **2004**, *5*, 232.
[17] NIST Cold Neutron Research Facility, NG3 and NG7 30-m. SANS Instruments Data Acquisition Manual, January **1999**.
[18] F. Horkay, M. Zrinyi, *Macromolecules* **1982**, *15*, 1306.
[19] H. Vink, *Europ. Polym. J.* **1971**, *7*, 1411.
[20] L. D. Landau, E. M. Lifshitz, "*Theory of Elasticity*", Pergamon Press, London **1986**.
[21] T. Tanaka, L. O. Hocker, G. B. Benedek, *J. Chem. Phys.* **1973**, *59*, 5151.
[22] J. R. C. van der Maarel, L. C. A. Groot, M. Mandel, W. Jesse, G. Jannink, V. Rodriguez, *J. Phys. II France* **1992**, *2*, 109.
[23] F. Horkay, P. J. Basser, A.-M. Hecht, E. Geissler, *J. Chem. Phys.* **2006**, *125*, 234904.
[24] S. S. Zakharova, S. U. Egelhaaf, L. B. Bhuiyan, C. W. Outhwaite, D. Bratko, J. R. C. van der Maarel, *J. Chem. Phys.* **1999**, *111*, 10706.

